Absolute and convective instability character of slender viscous vortices

Xie-Yuan Yin,[a] De-Jun Sun, and Ming-Jun Wei
Department of Modern Mechanics, University of Science and Technology of China, Hefei, Anhui, 230026, People's Republic of China

Jie-Zhi Wu
University of Tennessee Space Institute, Tullahoma, Tennessee 37388
and State Key Laboratory for Turbulence Research, Peking University, Beijing 100871, People's Republic of China

(Received 3 February 1999; accepted 28 December 1999)

Motivated by the need for effective vortex control, the character of absolute and convective instabilities (AI/CI) of incompressible and high-Mach number slender vortices with axial-velocity deficit is studied. Attention is focused on the disturbance modes which lead to the maximum absolute growth rate, and their dependence on flow conditions such as axial-flow profile, Reynolds number, and Mach number. A significant difference between the AI/CI and temporal-instability characters of the vortices occurs as the axial velocity deficit reduces. These theoretical results are applied to the flow region where vortex breakdown happens. It is found that the breakdown region is absolutely unstable, where waves are dominated by the spiral disturbance with lowest azimuthal wave number, in reasonable agreement with measurement. © *2000 American Institute of Physics.* [S1070-6631(00)02004-3]

I. INTRODUCTION

Slender vortices with jet-like or wake-like axial flow are known to appear very commonly in nature and technology. Their instability characters have been a subject of great interest for decades. While the normal-mode temporal instability (TI) of these vortices has been fully explored at least for incompressible flow (see the comprehensive review of Ash and Khorrami[1]), it was only recently that works on their absolute and convective instabilities [(AI/CI), for reviews of the theory see Huerre and Monkewitz[2] and Huerre and Rossi[3]] began to appear. Olendraru *et al.*[4,5] have used the normal-mode form of the inviscid linearized stability equations and a shooting method to study the AI/CI behavior of Batchelor trailing vortex. Based on different axial velocity, they divided the vortex into four classes: jet-like and wake-like, each has coflow(external and core streams are in same direction) or counterflow(external and core streams are in opposite direction). The AI/CI boundary was obtained for azimuthal wave numbers (in our notation; they used $m=-n$) $n=\pm 1, n=2,3$. By using direct numerical simulations (DNS) of linear impulse response, Delbende *et al.*[6] have obtained the AI/CI boundary similar to that of Olendraru *et al.*,[4,5] but with more azimuthal modes ($n=\pm 1, n=2,\ldots,7$). Also given are contours of different absolute growth rate for $n=1,2,3$. These results indicate that a swirling jet with coflow is convectively unstable, but AI can be triggered by a small amount of external counterflow (1.5% of center line velocity). In contrast, a swirling wake with coflow can transfer from CI to AI without the need for such triggering. The swirling wake with counterflow is, of course, also absolutely unstable. Loiseleux *et al.*[7] have considered the TI, AI, and CI of the Rankine vortex with plug-type axial flow. They found that for a swirling jet with zero external axial flow the transition from CI to AI first occurs at $n=2$ and $\mathrm{Ro}\simeq 0.62$, where Ro is the Rossby number, and this value of Ro is in good agreement with available measured and computed threshold Rossby numbers for vortex breakdown onset. Thus they proposed that the AI/CI transition boundary may provide a preliminary estimate for the critical Rossby number of vortex breakdown taking place. Sun[8] also attempted to study the AI/CI character of the Batchelor vortex using the viscous linear stability equations and a Chebyshev spectral collocation method, but he only considered the lowest azimuthal wave number n ($n=-1$ for jet-like and $+1$ for wake-like). The result was in qualitative agreement with those of Olendraru *et al.*[4,5] and Delbende *et al.*[6]

Our interest in the AI/CI character of swirling flows arises from our long-term goal of effective vortex control. Depending on the need, it is hoped to either enhance a favorable slender vortex or disrupt an unfavorable one by using steady or unsteady control devices. In particular, many experimental and numerical studies have shown that an unsteady forcing may cause an essential change of the flow state with very small power input (for recent work see Wu *et al.*,[9] Seifert and Park[10] and papers cited therein). A wide variety of flows can be controlled efficiently by this kind of forcing, and how to impose the forcing requires a clear understanding of the specific AI/CI character of the flow. Here are several different situations of practical interest.

For a convectively unstable flow, an upstream forcing can be very effective, as exemplified by forced shear layers.[11] In contrast, for an absolutely unstable flow, although an impulsive disturbance can be sufficient to trigger the growth of AI waves, for the control purpose it is useless since the imposed waves will be overwhelmed by the self-sustained AI waves. But a continuous forcing may signifi-

[a]Author to whom correspondence should be addressed; electronic mail: xyyin@ustc.edu.cn

cantly alter the location, structure, and/or even the dominant frequency (via frequency lock-in) of the AI waves, if some kind of resonance between the forcing and natural oscillations occurs. As shown in Wu *et al.*[9] and Seifert and Park[10] a forcing disturbance to boundary layer or separating shear layer (which are convectively unstable) can effectively control flow separation and separated flow associated with an AI region. An example more directly relevant to the present work is the experiment of Yao *et al.*,[12] who found that an upstream forcing spiral wave may delay the breakdown of a slender vortex, where the flow is absolutely unstable.

Moreover, if a finite absolutely unstable flow region is to be removed, it is usually believed that this can be achieved only by drastically changing the mean flow or boundary conditions.[13] However, it is interesting to note that some desired change of mean flow can also be realized by an unsteady forcing with small power input; Ming and Dai[14] have found that a zero-mass jet from an acoustic resonator may almost entirely eliminate the wake vortices behind a circular cylinder.

An examination of the above-mentioned examples (which are of course far from being a complete list) indicates that for controlling a vortex by unsteady forcing, it is important to know not only the AI/CI boundary, but also where to impose the forcing and what kind of disturbance modes possess the maximum absolute growth rate. These can also be answered at least partially by analyzing the AI/CI character of the vortex. Note that the optimal orientation of the imposed disturbance wave vector also has a very strong effect, but due to the use of the normal-mode method it cannot be identified, at least in the present work. But, for short-wave disturbances this optimal orientation can be obtained by using the geometric optics method,[15,16] which however cannot distinguish the AI/CI regions. Hence, these different approaches may complement each other as useful guidance to effective vortex control.

In this paper, therefore, we revisit the AI/CI character of viscous incompressible and compressible slender vortices, with emphasis on the above-mentioned issues important for control which are not covered in previous studies. We focus our attention on wake-like axial flows as they have richer instability phenomena compared with jet-like flows. After a brief review of theoretical formulation and numerical method (Sec. II), we study in Sec. III the incompressible AI/CI character, especially the effects of azimuthal wave number n, axial velocity deficit, and Reynolds number on inviscid AI/CI modes. (The pure viscous TI mode discovered by Khorrami[17] is very small at large Reynolds numbers and will not be addressed.) In Sec. IV we consider the effect of compressibility, limited to high Mach number flows. Then, in Sec. V we use these results to examine the AI character of a breakdown bubble, showing that the breakdown region is absolutely unstable and dominated by the most unstable low-n mode, i.e., a spiral mode, which has an almost constant frequency throughout the breakdown region. Finally, concluding remarks are presented in Sec. VI.

II. FORMULATION AND METHOD

The incompressible Batchelor vortex is the most commonly used model vortex in stability studies, and is also used in our study. Its velocity components (U,V,W) in cylindrical coordinates (r,θ,z) are given by

$$U=0, \quad V=\frac{q}{r}(1-e^{-r^2}), \quad W=W_\infty-W_d e^{-r^2}, \tag{1}$$

where W_∞ is the axial velocity as $r\to\infty$ and W_d is the maximum axial-velocity deficit or excess occurring at $r=0$. In TI analysis it is sufficient to take $W_\infty=0$ and $W_d=-1$ (a jet-like axial flow), since the temporal growth rate of disturbances is invariant under Galilean translation and coordinate inversion. The AI/CI character of a flow is not Galilean invariant, and a distinction of the AI/CI feature between jet-like $(W_d<0)$ and wake-like $(W_d>0)$ axial flows is important.

Stott and Duck[18] have proved that, if for a slender vortex $U(r),V(r),W(r)$ are much smaller than a uniform axial velocity, and if the Mach number defined by $M=W_d/c_\infty$ is large, where c_∞ is the speed of sound at infinity, then (1) can be approximately applied to compressible flow. They showed that to the leading order this compressible Batchelor vortex has uniform temperature, density, and pressure across the vortex core:

$$T=1, \quad \rho=1, \quad P=\frac{1}{\gamma M^2}, \tag{2}$$

where γ is the ratio of specific heats. Evidently, compressible vortices satisfying (2) may occur only under some special circumstances. Nevertheless, the gross effects of Mach number can be examined within this approximation. An instability analysis based on exact compressible Navier–Stokes slender vortex solutions has also been conducted and will be reported separately.[19]

For simplicity we assume the vortex is locally columnar. We set $W_d=1$ in (1) and use it to normalize all velocity components. We use $r=1=0.892r_0$ as the length scale, where r_0 is the core radius where $V=V_{\max}$. Then q measures the strength of swirl and is related to the ratio of maximum azimuthal velocity $V_{\max}$ and the maximum axial velocity deficit W_d.

We disturb the basic flow (1) [plus (2) for compressible case] to

$$(\mathbf{u},p,T)=(u,v,w,p,T)$$
$$=(u',V+v',W+w',P+p',T+T'),$$

and introduce normal-mode disturbances as usual:

$$\{u',v',w',p',T'\}$$
$$=\{iF(r),G(r),H(r),P(r),\Theta(r)\}e^{i(kz+n\theta-\omega t)}, \tag{3}$$

where F, G, H, P, and T are disturbance amplitudes, ω is the circular frequency, and k and n are axial and azimuthal wave numbers, respectively. The AI/CI analysis is concerned with spatiotemporal mode, for which both k and ω are complex. Substituting (3) into the Navier–Stokes equations leads to standard linearized stability equations. These equations,

along with proper boundary conditions, can be found in Khorrami *et al.*[20] for incompressible flow and Khorammi[21] for compressible flow, which need not be repeated here.

According to the definition of AI/CI and Briggs–Bers criterion,[2,3] our task is to find the asymptotic temporal-growth rate at large time for the source of impulse. Mathematically, based on the steepest-descent integral, this amounts to finding points with vanishing group velocity $(d\omega(k)/dk)=0$, that is, the saddle points k^0 of the dispersion relation $\omega(k)$ in the complex k plane or, equivalently, its branch points ω^0 in the complex ω plane. k^0 and ω^0 at a saddle point are referred to as the absolute complex wave number and absolute complex frequency, respectively. ω_i^0, the imaginary part of absolute complex frequency, is the absolute growth rate. An unstable flow will be absolutely unstable if: at least one of the branch-point singularities of the dispersion relation lies on the upper half of the ω plane (i.e., some $\omega_i^0>0$); and, the saddle point obtained thereby is the coalescence of a downstream traveling wave $k^+(\omega)$ and an upstream traveling wave $k^-(\omega)$, which can be judged from the saddle-point diagram by checking whether $k^+(\omega)$ and $k^-(\omega)$ are from the upper and lower halves of the complex k plane. This is the so-called pinching requirement for the path integral of wave package on the k plane. Otherwise the unstable flow is convectively unstable.

We use the Chebyshev spectral collocation method[20] to compute the eigenvalues of stability equations. The resulting discrete equations constitute a generalized eigenvalue problem of a complex matrix and can be solved by *QZ* method.

In our computation $r_{\max}=100$, and the number of terms of truncated Chebyshev polynomials was $N=50-70$. Selected results are in very good agreement with those obtained by Khorrami[17] and Mayer and Powell.[22]

To find saddle points numerically, the most primary approach is to compute the complex values of ω at the equal-spacing grid points of the complex k plane and then draw the contours of ω_r and ω_i which form a set of orthogonal meshes when $d\omega/dk\neq 0$. Thus, from the mesh plot the location of saddles can be identified. The plot also makes it easy to verify the pinching requirement. However, this approach requires a great amount of computation. Another approach is to use iteration, for which a few methods have been designed.[13,23] In order to obtain faster convergence, we constructed a quadratic-function iteration directly for $d\omega/dk$. Given four initial values k_j, $j=1,2,3,4$, we compute numerically the corresponding frequencies ω_j, and assume

$$\frac{d\omega}{dk}=a(k-k_4)^2+b(k-k_4)+c, \tag{4}$$

i.e., we construct an interpolating function

$$\omega(k)=\frac{a}{3}(k-k_4)^3+\frac{b}{2}(k-k_4)^2+c(k-k_4)+d,$$

where a, b, c, and d can be easily obtained from ω_j and k_j. Then, from the definition of saddles, a quadratic equation follows from (4) with two new roots of k. Taking the root closer to k_4 as k_5, one may use k_2, k_3, k_4, k_5 as initial values for a new round of iteration until k_5 converges to k^0 and ω to ω^0.

In this paper, the graphic method is first used to find the saddles satisfying the pinching-point requirement for a given basic profile. The estimate of the most unstable saddle (largest ω_i^0 among saddles on the above-mentioned plot) which determines the AI/CI character is subsequently used as guess value in the direct iteration (4) in order to generate more accurate numerical results. For other parameter settings of the basic flow, iterative solutions are obtained by applying suitably small increments to swirl q and proceeding by continuation.

III. AI/CI CHARACTER OF A WAKE-LIKE BATCHELOR VORTEX

In this section we confine our attention to incompressible flow. The computed AI/CI character for a wake-like Batchelor vortex, as given in (1) and with W_∞, q, and n as parameters, is presented in the following. In our computation the range of these parameters is $0.2\leqslant q\leqslant 1.4$, $0.8\leqslant W_\infty\leqslant 1.4$, and $n=1,2,3,4,6,10$. The Reynolds number is defined as $\mathrm{Re}=W_d r_0/\nu$. In most of the computation Re was taken as 10^{20} so that the instability is entirely inviscid. For selected cases we reduce Re to look at its effect.

In searching for unstable modes of a vortex with jet-like axial flow, taking $n<0$ is necessary; while for a vortex with wake-like axial flow we need take $n>0$. This can be seen most directly from the sufficient condition of temporal instability in terms of the vorticity components Ω_z and Ω_θ of the basic flow for large k and $|n|$, given by Staley and Gall:[24]

$$kr\Omega_z+n\Omega_\theta<0, \tag{5a}$$

where $k>0$, $\Omega_z>0$, and n and Ω_θ can be either positive or negative. Inequality (5a) is actually the vorticity form of the Leibovich–Stewartson criterion,[25,26] and can be cast as

$$n\frac{dW}{dr}>k\frac{d\Gamma}{dr}\ (>0). \tag{5b}$$

Then $n>0$ follows from the fact that $dW/dr\geqslant 0$ for wake-like axial flow.

We remark that some of the results presented here contain the same kind of information as obtained by Delbende *et al.*[6] at a fixed Reynolds number of 667, who plot figures in a different way (compare their Fig. 11 with Figs. 1 and 2 below for $\mathrm{Re}=10^{20}$). Our results using the Chebyshev spectral collocation method are in good consistency with theirs using DNS of linear impulse response, indicating both methods are reliable. But we cast ours from the viewpoint of vortex control.

A. The effect of axial-velocity deficit

Figure 1 shows the absolute growth rate ω_i^0 vs q for $n=1,2$ and different W_∞. The $(+)$ signs in the figure are the maximum temporal growth rate $\omega_{i\max}=0.2424$ with $q(\omega_{i\max})=0.458$ at $n=1$ and $\omega_{i\max}=0.3138$ with $q(\omega_{i\max})=0.693$ at $n=2$.[22] Initially, an increase of q leads to a corresponding increase of ω_i^0, which then starts to decrease

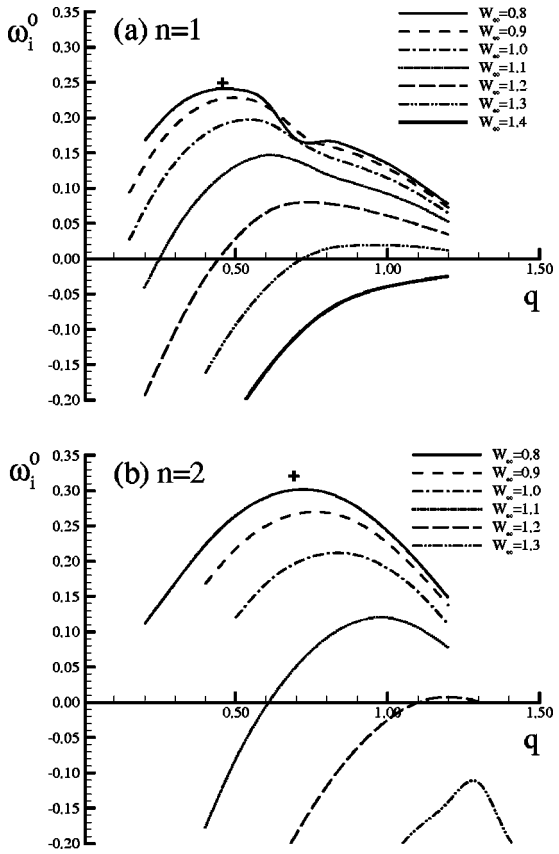

FIG. 1. The variation of absolute growth rate ω_i^0. The plus (+) symbol indicates the maximum temporal growth rate $\omega_{i\max}$ (a) $n=1$; (b) $n=2$.

from a larger q. Thus, for each pair of (W_∞, n), there is a maximum ω_i^0, which is denoted by $\omega_{i\max}^0$ and associated with a $q(\omega_{i\max}^0)$ not coinciding with $q(\omega_{i\max})$. From Fig. 1 it is evident that the axial flow has a strong effect on the AI/CI character of the vortex. The absolute growth rate reaches the largest value when there is a reverse flow ($W_\infty=0.8$), and this rate reduces as the axial velocity deficit does (W_∞ increases). Note that at $W_\infty=0.8$ and 0.9 for $n=1$ the ω_i^0-q curve has a valley, the possible mechanism of which will be discussed in Sec. III D.

Between temporal instability and AI/CI there must be[2]

$$\omega_{i\max}(n) \geqslant \omega_{i\max}^0(W_\infty, n) \quad \text{for all } W_\infty. \tag{6}$$

Hence, as W_∞ further decreases from 0.8, the trend of $\omega_{i\max}^0$ variation must be reversed. This already occurs for $W_\infty=0.8, n=1$ in a small range of q around 0.7. Therefore, a vortex with $W_\infty=0.8$ (and $q<1.5$, say), is close to the most absolutely unstable state.

When $W_\infty=1.1$, for about $q\leqslant 0.25$ the vortex becomes convectively unstable. For $W_\infty \geqslant 1.33$, i.e., smaller axial-velocity deficit, in the whole computed range of q the vortex is always convectively unstable. This should be the case far downstream in a trailing vortex. This result is also in qualitative agreement with the numerical simulation of Ragab and Sreedhar[27] for a Batchelor vortex with $n=1$, which shows that after a long time the initial disturbance tends to disappear and the flow recovers a laminar state (in their DNS result there is $W_\infty=1.35$ at $t=57$ and $W_\infty=1.7$ at $t=118$).

B. The effect of azimuthal wave numbers

Figure 2 compares the ω_i^0-q plots at different n and W_∞. For $W_\infty=0.8, 0.9$ [(Figs. 2(a) and 2(b)], the maximum growth rate $\omega_{i\max}^0(W_\infty, n)$ increases monotonically as n, somewhat similar to the trend of TI. But, for $W_\infty=1.0$ [(Fig. 2(c)], i.e., $W=0$ at $r=0$ (a stagnation point), the largest $\omega_{i\max}^0$ appears at $n=2$, after which it reduces. For $W_\infty \geqslant 1.1$, then, the largest $\omega_{i\max}^0$ moves to $n=1$. Therefore, the temporal analysis gives quite the same prediction of maxi-

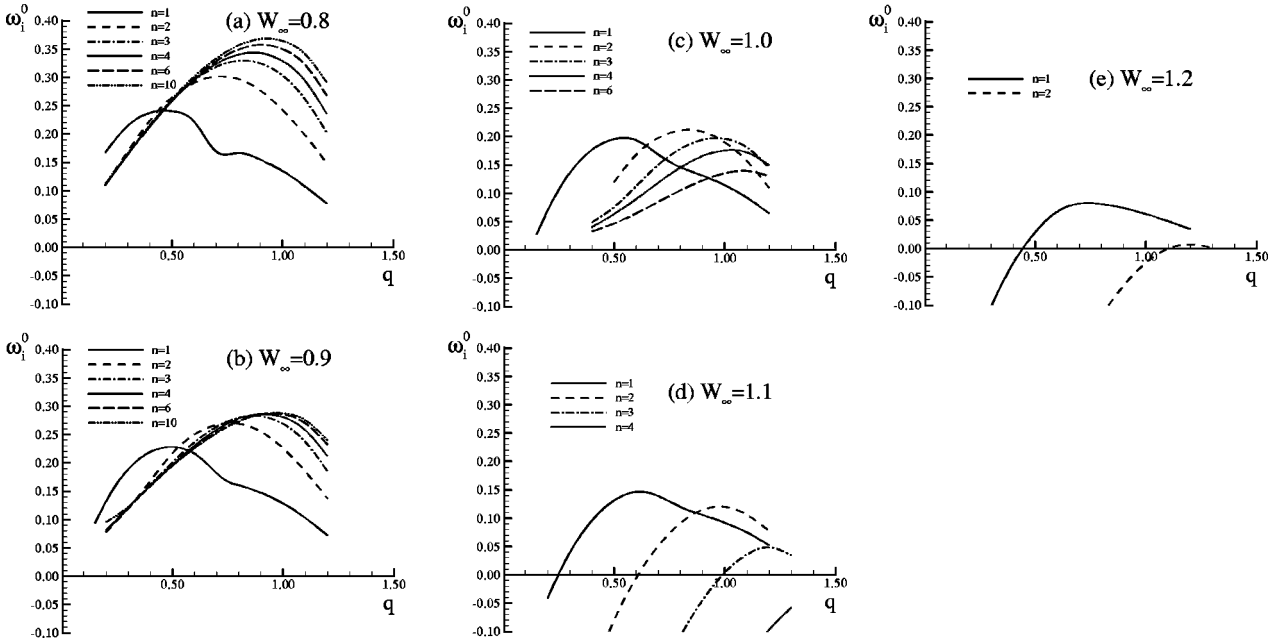

FIG. 2. The variation of absolute growth rate ω_i^0 as q for different azimuthal wave numbers. (a) $W_\infty=0.8$; (b) $W_\infty=0.9$; (c) $W_\infty=1.0$; (d) $W_\infty=1.1$; (e) $W_\infty=1.2$.

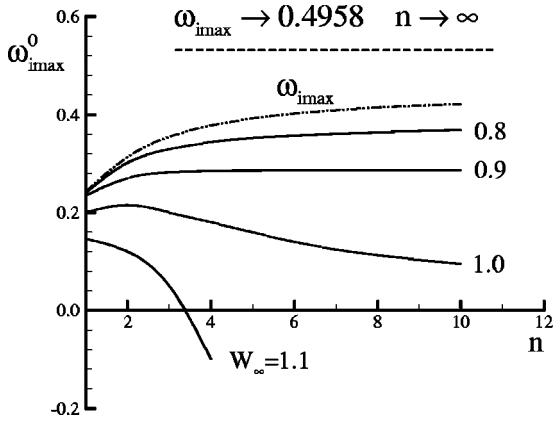

FIG. 3. The variation of maximum absolute growth rate as azimuthal wave number. The dash line shows the maximum temporal growth rate.

mum growth rate as AI/CI only if the axial-velocity deficit is so strong that a reversed flow appears. For a weak axial-velocity deficit, the dominant absolute instability waves are bending modes with relatively long axial wavelength, and disturbances with larger azimuthal wave numbers are more frequently proven to becoming convectively unstable.

In Fig. 3 we summarize the above-mentioned finding by plotting the variation of $\omega^0_{i\max}$ as n (solid lines). Also shown (double dot-dash lines) is the corresponding maximum temporal growth rate $\omega_{i\max}$ for comparison, taken from Mayer and Powell[22] and Table 8.2.1 of Ash and Khorrami.[1] It has been found that $\omega_{i\max}$ and corresponding q approaches a limiting value as $n\to\infty$ (shown on top of the figure): $\omega_{i\max}\to 0.4958$ and $q(\omega_{i\max})\to 0.871$.[22,25] We see that the variation of $\omega^0_{i\max}$ as n has the same qualitative feature as $\omega_{i\max}$ for $W_\infty<1.0$, but this is no longer so when $W_\infty\geqslant 1.0$. Clearly, for weak axial-velocity deficit the AI/CI prediction deviates more from the TI prediction. It is also seen that as the axial deficit velocity decreases (W_∞ increases), to reach $\omega^0_{i\max}$ one needs a larger q. We found that (not shown) the absolute growth rate ω^0_i at $q(\omega_{i\max})$ is *not* the maximum value and differs from $\omega^0_{i\max}$ increasingly as W_∞ increases.

C. Eigenfunctions

Figure 4(a) shows the radial variation of the amplitude of eigenfunctions $F(r)$, $G(r)$, $H(r)$, and $P(r)$ for $W_\infty=0.8$, $n=1$, and $q=1.0$. The eigenfunction of pressure disturbance is normalized by its maximum amplitude, and that of velocity disturbance by the maximum amplitude of the radial component. Figure 4(a) indicates that the peak amplitude of pressure disturbance occurs at about $0.35r_0$ ($r_0=1.122$ is the core radius), while the peak radial and azimuthal velocity disturbances locate at the vortex axis. The peak axial velocity disturbance is at $0.35r_0$ and slightly higher than the radial and azimuthal ones. From the figure it is also seen that significant disturbance energy extends to about $r=5$.

Figure 4(b) shows a case with large n: $W_\infty=0.8$, $n=10$, and $q=1.0$, which has the highest absolute growth rate within the range of our computation. Compared to Fig. 4(a), the difference is evident. The axial and radial velocity disturbance amplitudes are much larger than the azimuthal one, and their peaks move away from the vortex axis. Most remarkably, for this short-wave ($n=10, k_r=5.371$) disturbances are strongly amplified within the narrow vortex core, but quickly annihilated outside the core. This is in qualitative agreement with our recent finding that an initial short-wave disturbance located at $0.7r_0$ of a strained Q vortex[16] has maximum amplification.

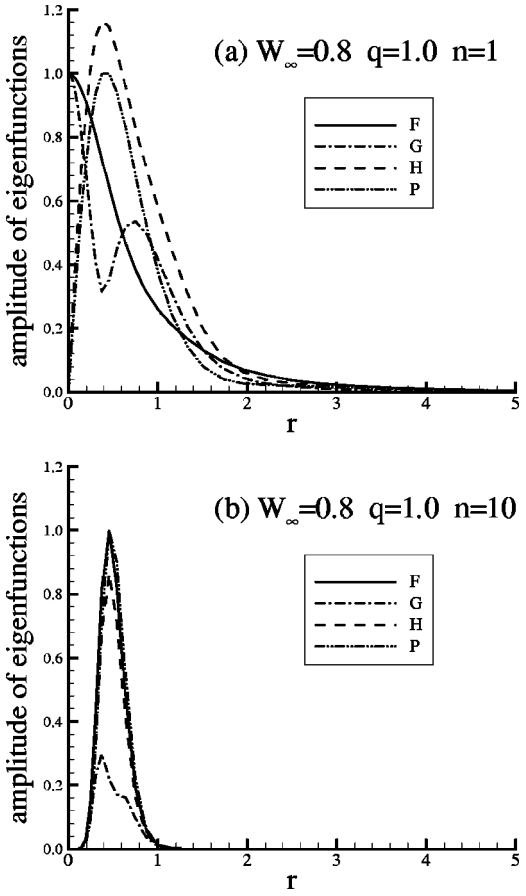

FIG. 4. Eigenfunctions $F(r)$, $G(r)$, $H(r)$, and $P(r)$ for $W_\infty=0.8$, $q=1.0$. (a) $n=1$; (b) $n=10$.

D. Effect of viscosity on inviscid modes

Figure 5 shows ω^0_i and ω^0_r (real part of absolute complex frequency) versus q for Re=5000, 500, 200, and 100 with $n=1$, $W_\infty=1.0$. It is seen that ω^0_i quickly decreases as viscosity increases. Figure 6, depicting the Re dependence of ω^0_i, shows that the effect of viscosity on inviscid modes is to enhance the stability. Also shown is the Re-dependence of absolute frequency ω^0_r. An increase of Re causes the complex ω^0 to quickly approach its inviscid value. It is of interest to see from Figs. 5 and 6 that the absolute frequency is smaller for less viscous flow, and in a range of smaller q, the dependence of absolute frequency on Reynolds number is not monotonic.

Figure 7 shows the effect of viscosity on $\omega^0_{i\max}$ for $W_\infty=0.8$ and 1.0, which exemplifies the viscous correction of the result of Fig. 3. Note that for $W_\infty>1.0$, Fig. 3 indicates that $\omega^0_{i\max}$ is already a monotonic decreasing function of n.

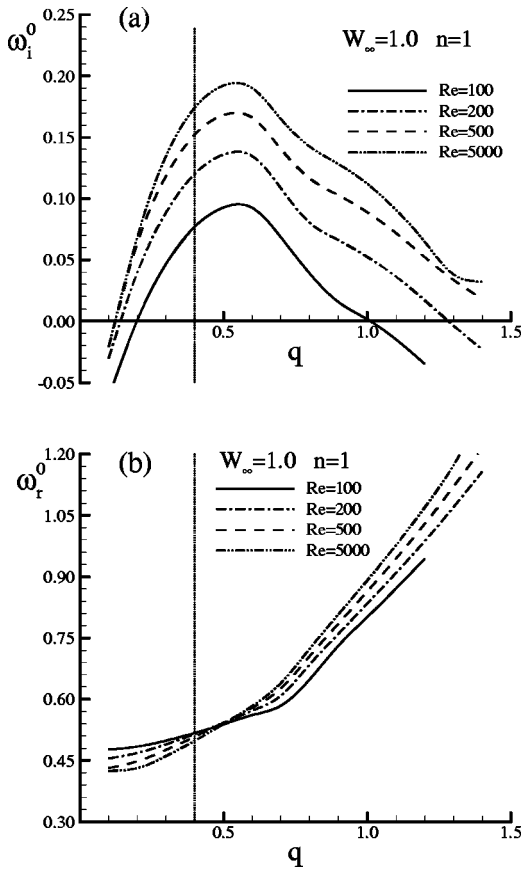

FIG. 5. The variation of (a) absolute growth rate ω_i^0 and (b) absolute frequency ω_r^0 as q for different Reynolds numbers. $W_\infty=1.0$, $n=1$.

We see from Fig. 7 that the viscosity damps out all waves with large n. The viscosity can even make the flow transition from AI to CI for large n, which could be a useful feature in vortex control.

The effect of viscosity on AI/CI boundary is shown in Fig. 8 for $W_\infty=1.1$ and $n=1$, 2, 3. A narrower AI region is moved to larger q and Re as n increases from 1. Note that there exists a critical Reynolds number $\mathrm{Re}_{cr}(W_\infty,n)$, such that for given axial velocity and azimuthal wave number, the flow is always CI

$$\text{if } \mathrm{Re}<\mathrm{Re}_{cr} \quad \text{for all } q.$$

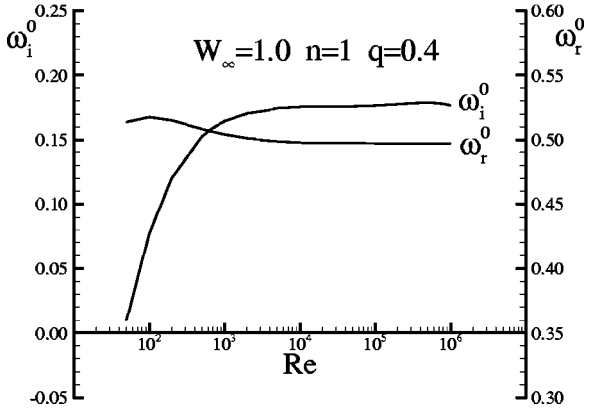

FIG. 6. Effect of viscosity on ω_i^0 and ω_r^0. $W_\infty=1.0$, $q=0.4$, $n=1$.

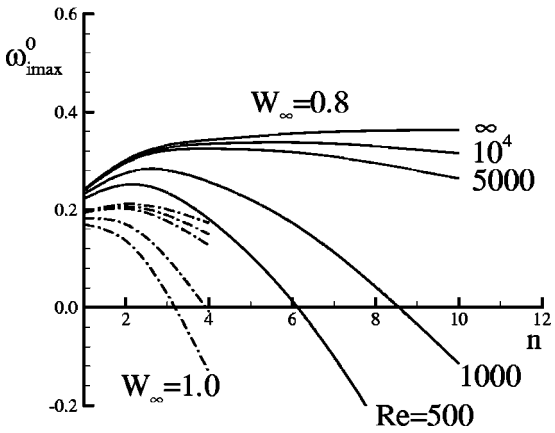

FIG. 7. Viscous effect on absolute growth rate with $W_\infty=0.8$ (solid lines) and 1.0 (broken lines).

Similarly, the swirling ratio of inviscid flow, say $q_{\mathrm{inv}}(W_\infty,n)$, serves as a critical value, such that for given axial velocity and azimuthal wave number, the flow is always CI

$$\text{if } q<q_{\mathrm{inv}} \quad \text{for all Re.}$$

As noticed by Khorrami,[28] viscosity has a complicated effect on the $n=1$ mode. His TI computation indicates that eigenmode switching may occur near the upper neutral boundary. Namely, the ω_i curve of the second eigenmode may go across the first one to become most unstable. This phenomenon also happens in AI/CI. Since our concern is mainly the maximum growth rate, we did not distinguish different eigenmodes and the curves in Fig. 5 are actually the envelopes of all eigenmodes. However, the effect of eigenmode switching can still be seen from the sign change of curvature of the curves. This eigenmode switching is much more apparent in multicell vortices, as Khorrami[29] found in a pipe flow with porous wall. Our recent instability study of unbounded incompressible and compressible Sullivan vortex also clearly shows the same phenomenon.[19] In fact, eigenmode switching may occur not only in viscous flow but also in inviscid flow. In Figs. 1 and 2 some of the ω_i^0–q curves already have a kink. In their TI study, Mayer and Powell[22] describe this kind of ω_i kink on (k,q) plane near $q=0.7$

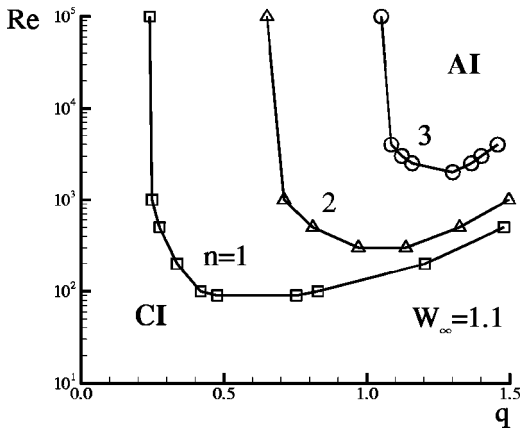

FIG. 8. Viscous AI/CI boundary with $W_\infty=1.1$.

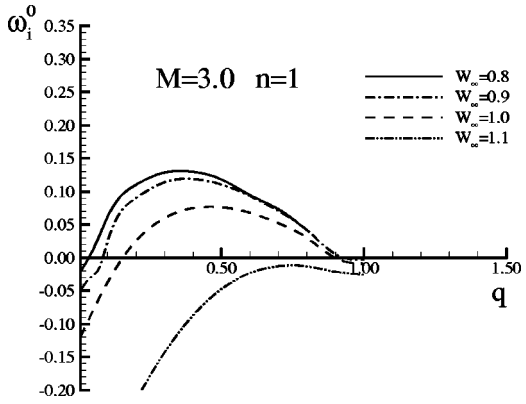

FIG. 9. Effect of axial velocity deficit on ω_i^0 for $M=3.0$ and $n=1$.

(their Fig. 3) as a two-lobed structure, in agreement with that appearing in our Figs. 1 and 2. It is likely that such kinks are also due to eigenmode switching.

IV. EFFECT OF HIGH MACH NUMBER

We now briefly consider the AI/CI character of a high-M Batchelor vortex. We chose $\gamma=1.4$, $\lambda=-2\mu/3$, $Pr=0.72$ for ratio of specific heats, second viscosity, and Prandtl number, respectively, and fix $\mathrm{Re}=1000$ except when we study the viscous effects.

Like the incompressible case, the axial velocity strongly influences the AI/CI character of compressible Batchelor vortex, as shown in Fig. 9. The absolute growth rate ω_i^0 is largest when there is a reverse flow ($W_\infty=0.8$), and reduces more quickly than incompressible flow (Fig. 1) as axial velocity deficit decreases.

Figure 10 shows the effect of azimuthal wave number on AI/CI. Contrary to incompressible flow, the maximum absolute growth rate for $W=1.0$ occurs at $n=1$ rather than $n=2$ [see Fig. 2(c)]. Its reduction with increasing n becomes more appreciable as the Mach number increases.

Figure 11 is the AI/CI boundary on the (M,q) plane. The $n=1$ mode has the largest AI region. The convectively unstable region is enlarged as n increases. On the other hand, the flow becomes less unstable when Mach number increases. The ω_i^0 contours are shown in Fig. 12.

Figure 13 is of special interest for vortex control, which shows the effect of swirling ratio q on AI/CI in supersonic flow. The swirl can significantly enhance the absolute growth rate. As Mach number increases to hypersonic regime (up to $M=8$) this effect still exists but is weaker and confined to a smaller interval of q. In particular, in a supersonic combustion chamber, say, there is an optimal swirling ratio $q_{\mathrm{opt}}(M)$ for the strongest enhancement of mixing. From Fig. 13 we see that $q_{\mathrm{opt}}\simeq 0.5$ for $M=2-3$, and $q_{\mathrm{opt}}\simeq 0.3$ for $M>5$.

V. ABSOLUTE INSTABILITY IN VORTEX BREAKDOWN

Several researchers have noticed that the flow in a vortex breakdown region is absolutely unstable.[4–6] A vortex-breakdown pattern may contain a recirculation region (axisymmetric bubble) or a sudden tilting of vortex axis without

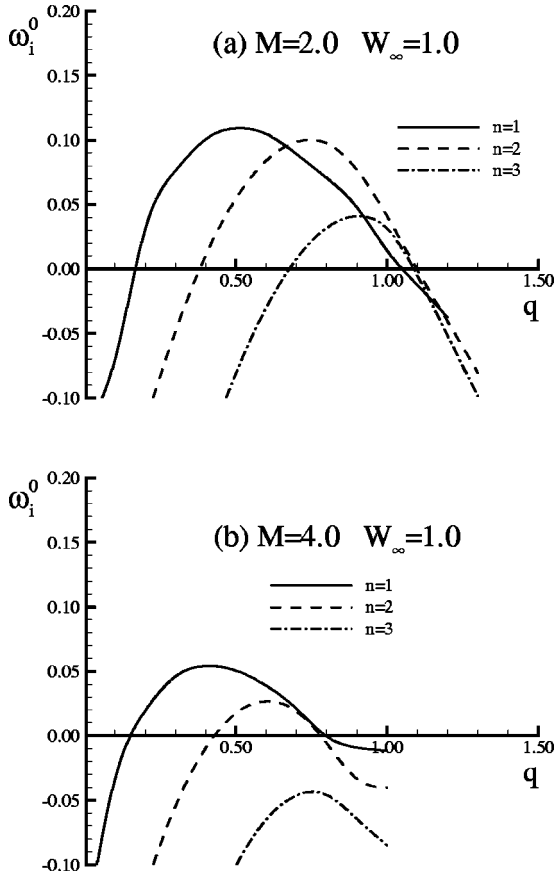

FIG. 10. Effect of azimuthal wave numbers. (a) $M=2.0$. (b) $M=4.0$.

reversed flow (spiral breakdown). For the former we have $W_\infty<1$ in terms of the Batchelor vortex model, and Figs. 2(a) and 2(b) indicate that the flow there should be absolutely unstable. This is confirmed by our computation based on the experimental data of Garg and Leibovich.[30] The result is listed in Table I, indicating that for all cases the flows in the near wake of breakdown bubble are indeed absolutely unstable. We also computed the AI/CI character using the experimental data of Benay, and of Pagan and Solignac (taken from Figs. 40 and 11 of Delery,[31] respectively), by fitting their velocity profiles by a modified version of (1).

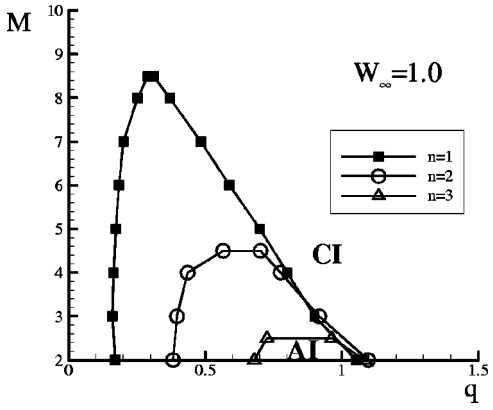

FIG. 11. Compressible AI/CI boundary.

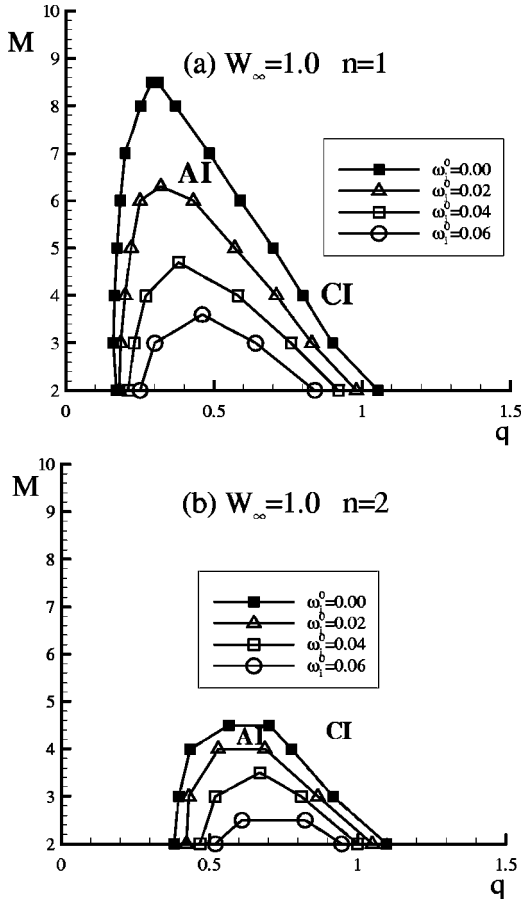

FIG. 12. Contours of absolute growth rate on (M,q) plane. (a) $W_\infty=1.0$, $n=1$; (b) $W_\infty=1.0$, $n=2$.

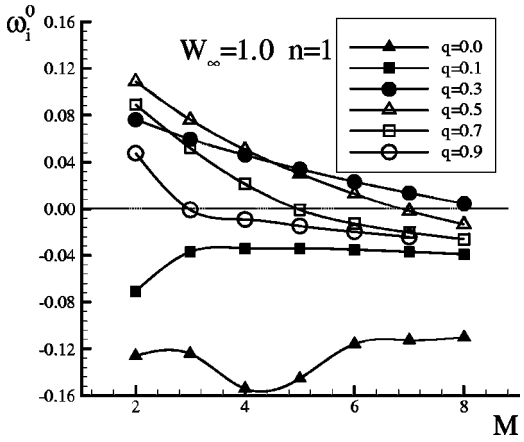

FIG. 13. The variation of absolute growth rate ω_i^0 as M for different q.

Once again the flows were found absolutely unstable. These tests strongly suggest that the absolute instability should be a common character in vortex breakdown.

In what follows we combine the general results of preceding sections and experimentally measured velocity profiles to further explore the character of dominant absolute frequency. Before proceeding, however, the inherent limitations of the present AI/CI approach, based on locally columnar assumption and using normal-mode decomposition (3), have to be restressed. First, due to inequality (6), it is impossible to find any unstable modes which are excluded by TI. Thus, except for small purely viscous modes, we cannot consider the key role of unstable axisymmetric disturbances in bubble-type breakdown as found by Wang and Rusak,[32,33] or the unstable spiral disturbances for $q>1.6$ as found by Tromp and Beran.[34] Second, we cannot decide if a vortex is globally stable or unstable even if a finite AI region is identified. Ultimately, vortex breakdown is a nonlinear bifurcation of the solutions of the Navier–Stokes equation or Euler equation (e.g., Wang and Rusak[35] and review therein), which can by no means be completely treated within any linear theory including AI/CI. Nevertheless, the correspondence between the concept of AI/CI and subcritical/supercritical states observed in the breakdown region strongly suggests that a vortex breakdown region must have some special AI character, which could lead to further understanding of the role of the unstable spiral waves downstream of breakdown.[30,36]

We first ask whether the AI theory can predict the dominant frequency in a breakdown bubble. Based on the experiment of Garg and Leibovich,[30] Tsai and Widnall[37] did a TI analysis to test a concept proposed by Bilanin[38] that in a breakdown region waves are trapped with vanishing group velocity. They found no support for this concept and concluded that the observed oscillations in the bubble are related to the local TI of the flow rather than its wave propagation characteristics. However, from the AI/CI point of view the group velocity C_g should be computed in the complex k plane. Thus, for trapped waves there is

$$C_g=\frac{d\omega}{dk}=\frac{x}{t}=0 \quad \text{for complex } \omega,k, \tag{7}$$

TABLE I. AI character in near wake of breakdown based on experimental profiles of Garg and Leibovich (Ref. 30).

Case	Re[a]	W_∞/W_d	q	k_r^0	k_i^0	ω_r^0	ω_i^0
1	9892	1.066	1.140	1.659 922	−0.563 106	3.556 942	0.242 629
2	9577	1.094	1.037	1.433 490	−0.804 143	2.919 500	0.244 768
3	7196	1.035	1.094	1.630 081	−0.547 424	3.143 451	0.270 133
4	5575	1.151	1.182	1.374 675	−0.724 399	3.766 633	0.156 573
5	4830	1.036	1.086	1.600 400	−0.568 426	3.081 507	0.264 991
6	4684	1.064	0.965	1.144 451	−0.705 080	2.293 895	0.226 299

[a]Here the Reynolds number is defined as $\mathrm{Re}=W_d a(z)/\nu$, where $a(z)$ is the radius of the vortex tube at the measurement station.

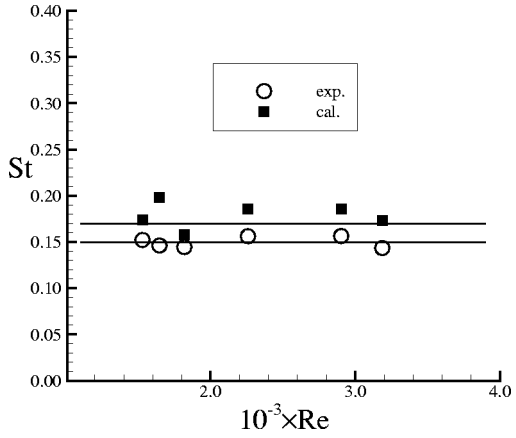

FIG. 14. Dominant Strouhal numbers in a breakdown bubble. St=0.171: theoretical prediction. St=0.15: average of measured values (Ref. 30).

rather than $c_g = d\omega_r/dk = 0$ with real k as Tsai and Widnall computed. Now from (7) we may obtain the corresponding absolute frequency f^0 for given W_∞, q, and n.

To choose these parameters, we first note that for Re $= W_d r_0/\nu = 1000-3000$ (in the range of the experiment of Garg and Leibovich[30]) low-frequency modes are dominant. When $W_\infty = 0.8$, the $n=2$ mode has the largest $\omega^0_{i\max}$; but as W_∞ slightly exceeds 0.9, the $n=1$ mode starts to dominate. Garg and Leibovich[30] reported that the dominant mode is $n=1$, which we now follow. They also found that the dominant frequency varies only slightly along the axis inside the bubble, and is in excellent agreement with the frequency at which the rear portion of the single-tailed bubble rotates about the axis. Indeed, for $q=1.0$ and $n=1$, we found as W_∞ varies from 0.8 to 1.0, f^0 only changes by 12%. Therefore, we may assume that this f^0 is also dominant inside the bubble. This assumption makes a simple comparison possible. Note that it is well known that the breakdown position may also oscillate with an even much lower frequency and almost constant amplitude; but this neutral wave is unlikely to be relevant to our discussion.

Next, the swirling flow inside the bubble is evidently a spatially developing flow, and if the spatial development is weak there exists a selection criterion for accurately predicting the global instability frequency.[2,3] Due to the limitation of the locally columnar assumption, however, a less accurate approach has to be adopted here. We follow a speculation of Koch,[39] that the dominant frequency could be determined from an ω^0 at the boundary of AI and CI regions, for which $\omega^0_i = 0$. We found that when Re=1000 and $(W_\infty, q) = (1.3, 0.935)$, there is $\omega^0_{i\max} = 0$. This gives an estimate of the dominant Strouhal number

$$\mathrm{St} = \frac{1.122\omega^0_r}{2\pi} = 0.171.$$

Figure 14 plots the computed Strouhal numbers based on experimental velocity profiles,[30] which are indeed around St $=0.17$, indicating the approximate feasibility of Koch's speculation and the approximate constancy of St across the AI region. In Fig. 14 are also plotted the measured Strouhal numbers,[30] yielding an averaged value of 0.15. Considering the fact that in a recirculating bubble the interaction of the flow at different z stations is strong, our result based on locally columnar-flow assumption is satisfactory.

Corresponding to the dominant ω^0_i there is naturally a dominant absolute axial wave length λ^0 (nondimensionalized by r_0), defined as

$$\lambda^0 = \frac{2\pi}{1.122 k^0_r}.$$

It is of also interest to ask whether λ^0 is somewhat correlated with the length scale of breakdown bubble. Assuming a constant St, for given W_∞ and n we can find the corresponding values of q, and hence λ^0. The result is listed in Table II for St=0.171 and 0.15. We see that when $n=1$ and St=0.171, as W_∞ varies from 0.8 to 1.3, λ^0 increases from 10 to 15.1. This interval shifts to (9.5, 11.6) if St=0.15 is used. At moderate to high Reynolds numbers, experimental results and numerical solutions indicate the bubble length L/r_0 varies from about 5 to 8.[31,34,40] Considering the fact that the AI region extends behind the bubble and λ^0 is merely a characteristic scale, this comparison is also reasonable. It should also be stressed that the length of a basically axisymmetric bubble cannot be solely determined by a dominant spiral wavelength.

VI. CONCLUDING REMARKS

Within the range of linearized normal-mode approach, the AI/CI theory represents a significant advance from the traditional TI analysis and provides much more information of use for vortex control. Our application of this theory to viscous incompressible and high-M slender vortex with axial-velocity deficit reveals several important features.

The AI/CI character has a strong dependence on the axial flow profile. First, in the unstable regime, the vortex is mostly convectively unstable when the W profile is jet-like,

TABLE II. Variation of q and λ^0 in breakdown region by assuming constant dominant St and $n=1$ (A) based on the criterion proposed by Koch (Ref. 39). (B) based on measured mean frequency.

(A) $\omega^0_r = 0.961$	W_∞	1.3	1.2	1.1	1.0	0.9	0.8
i.e.,	q	0.935	0.96	1.01	1.07	1.12	1.18
St=0.171	λ^0	15.14	12.727	11.50	10.45	10.43	10.0
(B) $\omega^0_r = 0.84$	W_∞	1.29	1.2	1.1	1.0	0.9	0.8
i.e.,	q	0.70	0.78	0.86	0.92	0.98	1.05
St=0.15	λ^0	11.55	10.18	10.57	10.04	9.54	9.51

but easily becomes absolutely unstable when the W profile is wake-like. It is always absolutely unstable when there is a wake-like counterflow. Second, for strong axial velocity deficit with counterflow the AI/CI analysis gives almost the same prediction of temporal analysis, i.e., ω_i^0 increases as azimuthal wave number n, and the predicted maximum growth rate and dominant frequency are quite close to their TI values. But the reliability of the TI prediction declines for weak velocity deficit, where low wave-number modes become dominant. When $W_\infty \geqslant 1.1$, ω_i^0 always reaches maximum at $n=1$, the lowest spiral mode, and for this mode the AI region in parameter space is the largest. These results agree well with the finding of Delbende *et al.*[6]

Viscosity always damps inviscid modes, in particular high-azimuthal-wave-number modes. For a given basic flow profile the vortex cannot be absolutely unstable if the Reynolds number is below a critical value. The absolute frequency also has a nonmonotonic dependence on the Reynolds number.

In supersonic and hypersonic regimes, swirling can greatly enhance the absolute growth rate. The existence of optimal swirling number, which is Mach-number dependent, may serve to enhance supersonic mixing.

The AI/CI character of vortex breakdown forms a very interesting test of the theory in concentrated vortex flows. Our analysis confirms that in breakdown region the flow is absolutely unstable. The AI prediction on the dominant frequency and size of breakdown bubble agree reasonably with available experiments.

Within the framework of linear theory, the main limitations of the present work are: using the locally columnar-flow approximation and being confined to the Batchelor vortex model, and incapability of finding unstable non-normal modes. This may cause significant departure between theoretical prediction and experimental or numerical results in some situations, e.g., in a certain range of swirling level and when a recirculating region appears. Further work in an attempt to alleviate these limitations is being undertaken.

Finally, for achieving effective vortex control, understanding the instability character of the vortices is only the first step. The receptivity character is of more direct significance in particular for control with continuous forcing, of which a systematic study is highly desired.

ACKNOWLEDGMENTS

The present work is a part of a U.S.–China International Cooperative Research Program sponsored by National Science Foundation of the United States (under Grant No. INT-9511552) and National Natural Science Foundation of China. We are very grateful to Turgut Sarpkaya and Peter A. Monkewitz for valuable discussions and unpublished information. The authors also thank Fang-Lin Zhu and Lin-Bo Jiang for their help in preparing the paper and figures.

[1] R. L. Ash and M. R. Khorrami, ''Vortex stability,'' in *Fluid Vortices*, edited by S. I. Green (Kluwer, Dorcrecht, 1995), p. 315.
[2] P. Huerre and P. A. Monkewitz, ''Local and global instabilities in spatially developing flows,'' Annu. Rev. Fluid Mech. **22**, 473 (1990).
[3] P. Huerre and M. Rossi, ''Hydrodynamic instabilities in open flow,'' in *Hydrodynamics and Nonlinear Instabilities*, edited by C. Godreche and P. Manneville (Cambridge University Press, Cambridge, 1998).
[4] C. Olendraru, A. Sellier, M. Rossi, and P. Huerre, ''Absolute/convective instability of the Batchelor vortex,'' C. R. Acad. Sci., Ser. II b: Mec., Phys., Chim., Astron. **323**, 153 (1996).
[5] C. Olendraru, A. Sellier, M. Rossi, and P. Huerre, ''Inviscid instability of the Batchelor vortex: Absolute-convective transition and spatial branches,'' Phys. Fluids **11**, 1805 (1999).
[6] I. Delbende, J. M. Chomaz, and P. Huerre, ''Absolute/convective instabilities in the Batchelor vortex: A numerical study of the linear impulse response,'' J. Fluid Mech. **355**, 229 (1998).
[7] T. Loiseleux, J. M. Chomaz, and P. Huerre, ''The effect of swirl on jet and wake: Linear instability of Rankine vortex with axial flow,'' Phys. Fluids **10**, 1120 (1998).
[8] M.-Y. Sun, ''Absolute and convective instability of swirling flows,'' M.S. thesis, University of Science and Technology of China, Hefei, China, 1995.
[9] J.-Z. Wu, X.-Y. Lu, A. G. Denny, M. Fan, and J.-M. Wu, ''Post-stall flow control on an airfoil by local unsteady forcing,'' J. Fluid Mech. **371**, 21 (1998).
[10] A. Seifert and L. G. Pack, ''Oscillatory excitation of unsteady compressible flows over airfoils at flight Reynolds numbers,'' AIAA Pap. 99-0925 (1999).
[11] C.-M. Ho and P. Huerre, ''Perturbed free shear layers,'' Annu. Rev. Fluid Mech. **16**, 365 (1984).
[12] M. F. Yao, L. B. Jiang, J. Z. Wu, H. Y. Ma, J. Y. Pan, and H. J. Cai, ''Delaying vortex breakdown by waves,'' AIAA Pap. **89**, 1000 (1989).
[13] P. A. Monkewitz and K. D. Sohn, ''Absolute instability in hot jet and their control,'' AIAA Pap. **86**, 1882 (1986).
[14] X. Ming and C. H. Dai, ''A new phenomenon of acoustic streaming,'' in Proceedings of the International Conference on Fluid Dynamic Measurement and Its Applications, edited by X. Shen and X. Sun, Beijing, China, 25–28 October 1989 (unpublished).
[15] A. Lifshitz and D. D. Holm, ''Short wavelength instabilities of incompressible three-dimensional flows and generation of vorticity,'' Phys. Lett. A **157**, 481 (1991).
[16] F.-L. Zhu, X.-Y. Yin, and J.-Z. Wu, ''Short-wave instability of strained swirling vortex,'' AIAA Pap. **99**, 0139 (1999).
[17] M. R. Khorrami, ''On the viscous modes of instability of a trailing line vortex,'' J. Fluid Mech. **225**, 197 (1991)
[18] J. A. K. Scott and P. W. Duck, ''The stability of a trailing-line vortex in compressible flow,'' J. Fluid Mech. **269**, 323 (1994).
[19] X.-Y. Yin, D.-J. Sun, and J.-Z. Wu, ''The instability of compressible Burgers and Sullivan vortices'' (unpublished).
[20] M. R. Khorrami, M. R. Malik, and R. L. Ash, ''Application of spectral collocation techniques to the stability of swirling flows,'' J. Comput. Phys. **81**, 206 (1989).
[21] M. R. Khorrami, ''Stability of a compressible axisymmetric swirling jet,'' AIAA J. **33**, 650 (1995).
[22] E. W. Mayer and K. G. Powell, ''Viscous and inviscid instabilities of a trailing vortex,'' J. Fluid Mech. **245**, 91 (1992).
[23] R. J. Deissler, ''The convective nature of instability in plane Poiseulle flow,'' Phys. Fluids **30**, 2303 (1987).
[24] D. O. Staley and R. L. Gall, ''Hydrodynamic instability of small eddies in a tornado vortex,'' J. Atmos. Sci. **41**, 422 (1984).
[25] S. Leibovich and K. Stewartson, ''A sufficient condition for the instability of columnar vortices,'' J. Fluid Mech. **126**, 335 (1983).
[26] K. A. Emanuel, ''A note on the instability of columnar vortices,'' J. Fluid Mech. **145**, 235 (1984).
[27] S. Ragab and M. Sreedhar, ''Numerical simulation of vortices with axial velocity deficits,'' Phys. Fluids **7**, 549 (1995).
[28] M. R. Khorrami, ''Behavior of asymmetric unstable modes f a trailing line vortex near the upper neutral curve,'' Phys. Fluids A **4**, 1310 (1992).
[29] M. R. Khorrami, ''A study of the temporal stability of multiple cell vortices,'' NASA-CR 4261 (1989).
[30] A. K. Garg and S. Leibovich, ''Spectral characteristics of vortex breakdown flow fields,'' Phys. Fluids **22**, 2053 (1979).
[31] J. M. Delery, ''Aspects of vortex breakdown,'' Prog. Aerosp. Sci. **30**, 1 (1994).
[32] S. Wang and Z. Rusak, ''On the stability of an axisymmetry rotating flow in a pipe,'' Phys. Fluids **8**, 1007 (1996a).
[33] S. Wang and Z. Rusak, ''The stability of noncolumnar swirling flows,'' Phys. Fluids **8**, 1017 (1996b).

[34]J. C. Tromp and P. S. Beran, ''The role of nonunique axisymmetric solutions in 3-D vortex breakdown,'' Phys. Fluids **9**, 992 (1997).
[35]S. Wang and Z. Rusak, ''The dynamics of a swirling flow in a pipe and transition to axisymmetric vortex breakdown,'' J. Fluid Mech. **340**, 177 (1997).
[36]S. Leibovich, ''Vortex stability and breakdown: Survey and extension,'' AIAA J. **22**, 1192 (1984).
[37]C. Y. Tsai and S. E. Widnall, ''Examination of group velocity criterion for breakdown of vortex flow in a divergent duct,'' Phys. Fluids **23**, 864 (1980).
[38]A. J. Bilanin, Ph.D. thesis, MIT, 1973.
[39]W. Koch, ''Local instability characteristics and frequency determination of self-excited wake flows,'' J. Sound Vib. **99**, 53 (1985).
[40]T. Sarpkaya (private communication).